# Genome-Wide Identification of *Francisella tularensis* Virulence Determinants[∇]

Jingliang Su,[1] Jun Yang,[1] Daimin Zhao,[1] Thomas H. Kawula,[2]
Jeffrey A. Banas,[1]† and Jing-Ren Zhang[1]*

*Center for Immunology and Microbial Disease, Albany Medical College, Albany, New York 12208,[1] and Department of
Microbiology and Immunology, School of Medicine, University of North Carolina, Chapel Hill, North Carolina 27599[2]*

*Francisella tularensis* **is a gram-negative pathogen that causes life-threatening infections in humans and has potential for use as a biological weapon. The genetic basis of the** *F. tularensis* **virulence is poorly understood. This study screened a total of 3,936 transposon mutants of the live vaccine strain for infection in a mouse model of respiratory tularemia by signature-tagged mutagenesis. We identified 341 mutants attenuated for infection in the lungs. The transposon disruptions were mapped to 95 different genes, virtually all of which are also present in the genomes of other** *F. tularensis* **strains, including human pathogenic** *F. tularensis* **strain Schu S4. A small subset of these attenuated mutants carried insertions in the genes encoding previously known virulence factors, but the majority of the identified genes have not been previously linked to** *F. tularensis* **virulence. Among these are genes encoding putative membrane proteins, proteins associated with stress responses, metabolic proteins, transporter proteins, and proteins with unknown functions. Several attenuated mutants contained disruptions in a putative capsule locus which partially resembles the poly-γ-glutamate capsule biosynthesis locus of** *Bacillus anthracis***, the anthrax agent. Deletional mutation analysis confirmed that this locus is essential for** *F. tularensis* **virulence.**

*Francisella tularensis* is a gram-negative, facultative intracellular bacterium that causes tularemia in humans and many other species (53). *F. tularensis* is divided into four subspecies or biotypes. *F. tularensis* subsp. *tularensis* (type A) and *F. tularensis* subsp. *holarctica* (type B) are the types mostly associated with human disease. The infection is naturally transmitted by multiple means, such as the bite of blood-sucking insects, handling infected animal carcasses, consumption of contaminated food or water, or inhaling infectious aerosols. Disease manifestation varies depending on the route of inoculation and ranges from ulceroglandular infection (entry through skin) to respiratory tularemia (inhalation). Among various forms of tularemia, respiratory tularemia has attracted the most attention because it may cause high mortality (up to 35%) in humans in the absence of antibiotic therapy (48). In addition, aerosolized *F. tularensis* can cause a large number of tularemia cases (11, 13). The infectious dose of *F. tularensis* in humans via the airborne route is as low as 10 organisms (48). *F. tularensis* was developed as a bioweapon by Japanese germ warfare units during World War II and later by the former Soviet Union and the United States because of its extreme infectivity, high virulence, and ease of dissemination (16). *F. tularensis* is listed as a category A potential agent of bioterrorism (16).

Despite the importance of this pathogen, the virulence mechanisms of *F. tularensis* are poorly understood. The ill-defined capsule (34, 60, 67), lipopolysaccharide (LPS) (61, 64, 74), and the genes involved in intramacrophage growth (42, 50, 69) are among a few known factors that can contribute to pathogenesis and virulence of *F. tularensis*. The recently sequenced genomes of three *F. tularensis* strains have predicted approximately 2,000 genes (40, 54), but many of the putative genes do not have assigned biological roles. *F. tularensis* live vaccine strain (LVS) is a type B derivative. LVS is relatively avirulent in humans but causes a lethal infection in mice that highly resembles human tularemia (2, 19). Thus, the mouse infection model with LVS has been extensively used to study *F. tularensis* pathogenesis and host response during tularemia. The LVS genome has been fully sequenced (GenBank accession no. AM233362).

The lack of genetic manipulation tools has been a major hurdle in understanding virulence determinants of this organism (53). Among the recent advancements in establishing genetic tools in *F. tularensis*, a Tn5-based transposon-transposase complex has been successfully used to generate random and stable insertion mutations in the chromosome of *F. tularensis* LVS (36). In this study, we have modified this mutagenesis technique to perform a genome-wide screening to identify virulence determinants of *F. tularensis* LVS by signature-tagged mutagenesis (STM). STM was originally developed to identify virulence factors in *Salmonella enterica* serovar Typhimurium by negative selection (33). This technique has been successfully used to identify virulence-associated genes in many other pathogens (10). Our STM screening work has led to the discovery of 95 *F. tularensis* genes that contribute to the survival of this pathogen in a mammalian host. Importantly, virtually all identified genes from *F. tularensis* LVS are also present in the genomes of other *F. tularensis* strains, including strain Schu S4 (40).

* Corresponding author. Mailing address: Center for Immunology and Microbial Disease, Albany Medical College, M/C 151, Room MS453, 47 New Scotland Avenue, Albany, NY 12208. Phone: (518) 262-6412. Fax: (518) 262-6161. E-mail: zhangj@mail.amc.edu.
† Present address: University of Iowa College of Dentistry, Iowa City, IA 52242.

## MATERIALS AND METHODS

**Bacterial strains and chemical reagents.** *F. tularensis* LVS was kindly provided by Karen Elkins. LVS and its derivatives were cultured with aeration in modified Mueller-Hinton broth (MHB) supplemented with 0.025% ferric pyrophosphate and IsoVitaleX (MHB) or on chocolate agar plates. When necessary, kanamycin (10 $\mu$g/ml) or hygromycin (200 $\mu$g/ml) was included in the broth and agar media for selection purposes. *Escherichia coli* strains DH5$\alpha$ and S17-1 were grown in Luria-Bertani broth or on Luria-Bertani agar plates and, when appropriate, ampicillin, kanamycin, and hygromycin were added to final concentrations of 100 $\mu$g/ml, 50 $\mu$g/ml, and 200 $\mu$g/ml, respectively. All ingredients for bacterial culture media and other chemicals used in this work were obtained from Sigma (St. Louis, MO) unless otherwise stated.

**Construction of tagged transposons.** The Tn5-based EZ::TN transposon in the pMOD3 plasmid (Epicenter, Madison, WI) was first modified by inserting a kanamycin resistance cassette in the PstI/KpnI sites. The kanamycin resistance cassette was amplified from the EZ::TN transposon (Epicenter) by PCR using primers Pr451 (5′-GGGTACCAAAGCCACGTTGTGTCTCAAA-3′) and Pr452 (5′-GCTGCAGGTCGACTCTAGAGGAT-3′). The resulting transposon was individually tagged with distinct 52-bp oligonucleotides by inserting these tags in the KpnI site of pMOD3. The tag sequences were amplified from the pID701t plasmids by PCR using primers Pr455 (5′-CAAGGTACCCATTCTAACCAAGCT-3′) and Pr456 (5′-GGGGTACCTACAACCTCAAGCT-3′). These tags were previously used to identify virulence determinants in *Streptococcus pneumoniae* by the STM approach (41) and were generously provided by Sauli Haataja. The sequences of the resulting transposon constructs were determined by DNA sequencing using the primer Pr457 (5′-ATTCAGGCTGCGCAACTGT-3′) based on the backbone sequence of pMOD3.

**Construction of tagged mutants in *F. tularensis* strain LVS.** The tagged transposons were released from pMOD3 by restriction digestion with PvuII, separated from the plasmid backbones in 1% agarose gels, and gel purified using the QiaQuick gel extraction kit (QIAGEN, Valencia, CA). The isolated transposon DNA fragments were mixed with the EZ::TN transposase (Epicenter) and incubated to form transposome complexes at −20°C for 2 to 4 days according to the supplier's instructions. The complexes were electroporated into LVS under the conditions described by Kawula et al. (36). The transformants were selected on chocolate agar plates containing kanamycin (10 $\mu$g/ml). The resulting colonies were individually cultured in MHB and preserved in MHB containing 20% (vol/vol) glycerol at −80°C for future characterization.

**DNA electrophoresis and Southern hybridization.** DNA cloning and manipulations were carried out according to standard methods (59). *F. tularensis* genomic DNA was prepared as described in "DNA sequencing and sequence analysis," below. For Southern hybridization with the STM strains, approximately 3 $\mu$g chromosomal DNA from each strain was digested with EcoRI and separated in a 1% agarose gel. All restriction enzymes and DNA standards used in this study were purchased from New England Biolabs (Beverly, MA). DNA was blotted to Hybond-N$^+$ nylon membranes (GE Healthcare BioSciences Corp., Piscataway, NJ) by the alkaline transfer method and hybridized with a digoxigenin (DIG)-dUTP-labeled DNA probe essentially as described elsewhere (45). The transposon-specific probe representing the 270-bp coding region of the kanamycin resistance cassette in the transposon was amplified from the tagged transposon with primers Pr626 (5′-ATAAATGGGCTCGCGATAATGTC-3′) and Pr627 (5′-GCGCATCAACAATATTTTCACCTG-3′) and the PCR DIG probe synthesis kit as described by the supplier (Roche, Indianapolis, IN). Sizes of DNA fragments were estimated based on DIG-labeled DNA molecular weight standards (Roche).

**Selection of transposon mutants in mice.** The tagged transposon mutants of strain LVS were individually cultured overnight in MHB. The cultures were centrifuged and resuspended to the same optical density at 600 nm ($OD_{600}$) in MHB. Equal volumes of the tagged mutants were pooled, supplemented with sucrose to a final concentration of 10% (wt/vol), and stored at −80°C as the input pools. The frozen stocks were later thawed in a 37°C water bath to determine the concentration of viable bacteria. For mouse infection, the frozen stocks of the STM pools with a predetermined concentration of viable bacteria were diluted to approximately $1.25 \times 10^5$ CFU/ml with sterile phosphate-buffered saline (PBS) for mouse infection.

Groups of four female BALB/c mice (6 to 8 weeks old; Taconic Farm, Germantown, NY) were each infected with a single-input pool by intranasal inoculation of 40 $\mu$l bacterial suspension (approximately 5,000 CFU). The mice were anesthetized with ketamine-HCl (Fort Dodge Animal Health, Fort Dodge, IA) and xylazine (Phoenix Scientific, St. Joseph, MO) in PBS immediately prior to infection. Portions of the inocula were diluted in PBS and spread on chocolate agar containing kanamycin (10 $\mu$g/ml) to verify the infection dose and to gen-

erate a DNA template of the input pool for PCR detection. The mice were sacrificed 7 days postinfection. The lungs, livers, and spleens were aseptically removed and homogenized using tissue strainers (Becton Dickinson) and plugs of 5-ml syringes. Each organ homogenate was diluted in 1 ml of sterile PBS and partially plated (100 $\mu$l of each homogenate) on chocolate agar containing kanamycin (10 $\mu$g/ml) to establish the output pool. The remaining portion of each organ homogenate was stored at −80°C as a backup source of the output pool. All animal infection procedures were in compliance with the guidelines of the Institutional Animal Care and Use Committee.

**Detection of recovered transposon mutants by PCR.** The presence of the tagged mutants in the input and output pools was detected by PCR essentially as described elsewhere (43). All bacterial colonies obtained with each of the input and output pools were washed off from agar plates with 5 ml sterile PBS. A portion of the bacterial suspension (1.5 ml) was pelleted by centrifugation, resuspended in 500 $\mu$l H$_2$O, boiled for 10 min to lyse the bacteria and liberate chromosomal DNA, and centrifuged to remove bacterial debris. The supernatants were used as DNA templates for PCR detection of the STM strains in the mutant pools. The remaining portion of the bacterial suspension was stored at −80°C as a backup source. Each input and output DNA template was tested in 41 PCRs, each of which contained a tag-specific primer and a common primer based on the kanamycin resistance cassette of the transposon. The tag-specific primers were synthesized based on our DNA sequence information for each of the tags (41). To compare the amplification profiles of the input and output pools for the same mutant sets, PCR products were separated in 1.2% agarose gels and visualized by staining agarose gels with ethidium bromide (2 $\mu$g/ml). An STM strain was considered to be attenuated for infection when no or substantially decreased PCR products were observed from the output pools of at least two mice compared with a positive PCR signal for the corresponding input pools. To avoid screening errors, strains with ambiguous results were rescreened in separate infection experiments and sometimes in separate pools.

**DNA sequencing and sequence analysis.** Transposon insertion sites in the LVS chromosome were determined by direct sequencing of genomic DNA using a transposon-specific primer Pr800 (5′-CGAGCCAATATGCGAGAACA-3′) essentially as described previously (55). Our experience suggested that the purity of the genomic DNA preparations was vital for the success rate of DNA sequencing. Briefly, a single STM strain was cultured in 10 ml MHB to an $OD_{600}$ of 0.8 to 1.0, pelleted by centrifugation, and resuspended in 567 ml TE buffer (0.01 M Tris-HCl, pH 8.0, 1 mM EDTA). The bacteria were lysed by adding 40 $\mu$l of 10% sodium dodecyl sulfate and 40 $\mu$l pronase (20 mg/ml) to the suspension and incubating for 1 h at 37°C. After mixing with 100 $\mu$l of 5 M NaCl, 80 $\mu$l of 0.7 M NaCl containing 10% (wt/vol) cetyltrimethylammonium bromide was added. The mixtures were incubated for 10 min at 65°C before proceeding to the standard phenol-chloroform extraction for final DNA purification (59). The purified genomic DNA was used as a template for automated DNA sequencing. The resulting DNA sequences were used to perform homology searches against the complete genome sequences of *F. tularensis* strains LVS (accession no. AM233362) and Schu S4 (40) (accession no. NC_006570). DNA and protein sequence analyses were performed using DNASTAR Lasergene v6.1 for Macintosh (Madison, WI).

**In vitro growth index.** The wild-type LVS and each of the attenuated mutants identified in the STM screening were individually cultured overnight in MHB, diluted to an $OD_{600}$ of approximately 0.050 with fresh MHB, and allowed to grow in the absence of antibiotic selection. The density of each culture was periodically monitored by optical absorbance ($OD_{600}$). The change of culture density for each mutant strain was compared with that of LVS to assess potential defects of the STM strains. The difference is expressed as the in vitro growth index (GI), which is defined by the ratio between mutant density change and LVS density change (mutant/wild type). The GI values at the 18-h time point are presented in Table 1, because all tested strains were apparently in the late log growth phase at this time, an optimal stage for detection of growth differences based on our experience. A GI value below or above 1 indicates the corresponding mutant had a slower or faster growth rate, respectively, under these conditions. We observed that *F. tularensis* mutants usually showed reproducible growth differences when their in vitro GI values differed from that of the parent strain by more than 0.3 (unpublished data). We empirically used this cutoff value to define the growth deficiency status of the STM strains.

**Complementation of disrupted *capB* and *capC*.** The wild-type *capB* and *capC* genes were PCR amplified from the LVS genomic DNA using primer pairs Pr884 (5′-AGACATATGACTACTTTGGATTTTTGGTTAATTG-3′)/Pr1103 (5′-TTGTGTCATATGAAAACTCCTTTAAATACCGGATCCATATTTTCTCCTG TTT-3′) and Pr886 (5′-AGACATATGGGATCCGTTAACGCTCTCGATAGG-3′)/Pr1104 (5-TTGTGTCATATGAAAACTCCTTTAAATACTTATATTCCT ACTATCTCAGGTCCAATTA-3′), respectively. The PCR products were

TABLE 1. *F. tularensis* LVS genes essential for lung infection identified by STM

| Function group and mutant ID[a] | ORF in LVS[b] | ORF in Schu S4[c] | Gene[d] | Predicted function[d] | No. of independent mutants[e] | In vitro GI[f] |
|---|---|---|---|---|---|---|
| Cell surface structures and membrane proteins | | | | | | |
| JS4512 | FTL_0009 | FTT1747 | | Outer membrane protein | 1 | 0.70 |
| JS3217 | FTL_0073 | FTT1676 | | Membrane protein | >5 | 0.89 |
| JS2802 | FTL_0421 | FTT0901 | tul4 | Lipoprotein, T-cell-stimulating antigen | 2 | 0.89 |
| JS4596 | FTL_0540 | FTT1568c | lpxB | Lipid A-disaccharide synthase | 1 | 1.00 |
| JS1430 | FTL_0589 | FTT1525c | | Hypothetical membrane protein | 2 | 0.92 |
| JS3023 | FTL_0592 | FTT1464c | wbtA | dTDP-glucose 4,6-dehydratase, LPS modification | 1 | 0.74 |
| JS2516 | FTL_0597 | FTT1459c | wbtF | NAD-dependent epimerase, LPS modification | 2 | 0.70 |
| JS4788 | FTL_0645 | FTT1416c | | Lipoprotein | 2 | 0.81 |
| JS2294 | FTL_1096 | FTT1103 | | Lipoprotein | 2 | 0.78 |
| JS1965 | FTL_1134 | NA | | Membrane protein | 2 | 0.60 |
| JS4709 | FTL_1328 | FTT0583 | fopA | Outer membrane-associated protein | >5 | 0.49 |
| JS1083 | FTL_1354 | FTT0759 | | Membrane protein | 4 | 0.46 |
| JS4622 | FTL_1414 | FTT0807 | capA | Transmembrane HSP60 family protein | 2 | 1.10 |
| JS2531 | FTL_1415 | FTT0806 | capC | Capsular polyglutamate biosynthesis protein CapC | 2 | 0.93 |
| JS2512 | FTL_1416 | FTT0805 | capB | Capsular polyglutamate biosynthesis protein CapB | 3 | 1.21 |
| JS1091 | FTL_1475 | FTT1314c | | Type IV pilus fiber building block protein | 2 | 0.57 |
| JS4638 | FTL_1678 | FTT0101 | | Membrane protein | 1 | 0.61 |
| Intracellular survival and stress response | | | | | | |
| JS1967 | FTL_0094 | FTT1769C | clpB | Endopeptidase Clp ATP-binding chain B | >5 | 0.46 |
| JS2797 | FTL_0111 | FTT1359c | iglA | Intracellular growth | 3 | 0.77 |
| JS4621 | FTL_0112 | FTT1358c | iglB | Intracellular growth | 2 | 0.96 |
| JS3579 | FTL_0113 | FTT1357c | iglC | Intracellular growth | 5 | 1.00 |
| JS3200 | FTL_0519 | FTT1606 | minD | Division inhibitor ATPase | 1 | 0.79 |
| JS2866 | FTL_0520 | FTT1605 | minC | Septum site-determining protein | 2 | 0.69 |
| JS1816 | FTL_0891 | FTT0623 | tig | Molecular chaperone | >5 | 0.43 |
| JS2466 | FTL_0892 | FTT0624 | clpP | ATP-dependent Clp protease subunit P | 1 | 0.90 |
| JS2488 | FTL_0893 | FTT0625 | clpX | ATP-dependent Clp protease subunit X | 2 | 0.72 |
| JS1838 | FTL_0894 | FTT0626 | lon | ATP-dependent protease Lon | >5 | 0.68 |
| JS1216 | FTL_1097 | FTT1102 | | Macrophage infectivity potentiator | 2 | 0.67 |
| JS4549 | FTL_1392 | FTT1471c | deaD | Cold shock DEAD box protein A | 4 | 0.64 |
| JS4653 | FTL_1473 | FTT1312c | uvrA | DNA excision repair enzyme, subunit A | 1 | 0.75 |
| JS2712 | FTL_1504 | FTT0721c | katG | Catalase | 2 | 0.70 |
| Metabolism and biosynthesis | | | | | | |
| JS1849 | FTL_0010 | FTT1748 | glpE | Thiosulfate sulfurtransferase | 1 | 0.95 |
| JS2839 | FTL_0193 | FTT0283 | cyoC | Cytochrome *O*-ubiquinol oxidase subunit III | 1 | 1.05 |
| JS3158 | FTL_0382 | FTT0881c | rocE | Amino acid permease | 2 | 0.39 |
| JS4576 | FTL_0387 | FTT0884c | aspC1 | Aspartate aminotransferase | 1 | 1.07 |
| JS2511 | FTL_0483 | FTT0413c | glgB | 1,4-α-Glucan branching enzyme | 1 | 0.93 |
| JS2367 | FTL_0485 | FTT0415 | glgC | Glucose-1-phosphate adenylyltransferase | 1 | 0.81 |
| JS3699 | FTL_0525 | FTT1600c | fumA | Fumerate hydratase | 2 | 0.56 |
| JS2301 | FTL_0584 | FTT1530 | fadB | Acyl-CoA-binding protein | 4 | 1.46 |
| JS4239 | FTL_0789 | FTT1165c | aspC2 | Aspartate aminotransferase | >5 | 0.71 |
| JS4275 | FTL_0846 | FTT1117c | | Isochorismatase hydrolase family protein | 1 | 0.62 |
| JS4467 | FTL_0960 | FTT0684C | sthA | Soluble pyridine nucleotide transhydrogenase | >5 | 0.89 |
| JS1239 | FTL_1240 | FTT0963c | aroG | Phospho-2-dehydro-3-deoxyheptonate aldolase | >5 | 0.34 |
| JS2226 | FTL_1266 | FTT0941c | lipP | Lipase/esterase | 1 | 0.89 |
| JS2758 | FTL_1273 | FTT0936c | bioF | 8-Amino-7-oxononanoate synthase | 1 | 0.77 |
| JS2559 | FTL_1274 | FTT0935c | bioC | Biotin synthesis | 1 | 0.95 |
| JS4610 | FTL_1275 | FTT0934c | bioD | Dethiobiotin synthetase | 5 | 0.90 |
| JS2717 | FTL_1419 | FTT0802 | cphB | Cyanophycinase | 1 | 0.90 |
| JS2632 | FTL_1553 | FTT0504c | sucC | Succinyl-CoA synthetase beta chain | 1 | 0.75 |
| JS2228 | FTL_1554 | FTT0503c | sucD | Succinyl-CoA synthetase alpha chain | 1 | 0.60 |
| JS2292 | FTL_1701 | FTT1631c | glpX | Fructose-1,6-bisphosphatase | >5 | 0.57 |
| Transcription, translation, and cell separation | | | | | | |
| JS3170 | FTL_R0003 | FTTr07 | 16S rRNA | 16S rRNA | >5 | 0.80 |
| JS3560 | FTL_R0004 | FTTt19 | tRNA-Ile | tRNA-isoleucine | 1 | 0.73 |
| JS3583 | FTL_0257 | FTT0346 | rpmJ | 50S ribosomal protein L36 | 1 | 0.41 |

TABLE 1—*Continued*

| Function group and mutant ID[a] | ORF in LVS[b] | ORF in Schu S4[c] | Gene[d] | Predicted function[d] | No. of independent mutants[e] | In vitro GI[f] |
|---|---|---|---|---|---|---|
| JS4647 | FTL_0428 | FTT0908 | *parB* | Chromosome partition protein B | 1 | 0.74 |
| JS3754 | FTL_0456 | FTT0390c | *rpsU1* | 30S ribosomal protein S21 | 1 | 0.79 |
| JS2299 | FTL_0616 | FTT1442c | *rpoA2* | DNA-directed RNA polymerase, α subunit | 1 | 0.50 |
| JS4292 | FTL_0768 | FTT1179 | *bipA* | GTP-binding translational elongation factor Tu and G family protein | 1 | 0.84 |
| JS3069 | FTL_0899 | FTT0631 | *hflX* | Protease, GTP-binding subunit | 1 | 0.77 |
| JS3240 | FTL_0903 | FTT0633 | *hflK* | Protease modulator | 1 | 0.59 |
| JS3165 | FTL_0928 | FTT0654 | *elbB* | DJ-1/PfpI family protein | 3 | 0.90 |
| JS3181 | FTL_0950 | FTT0675 | *rplY* | 50S ribosomal protein L25 | 3 | 0.90 |
| JS4305 | FTL_1030 | FTT1056c | *rluB* | Ribosomal large subunit pseudouridine synthase B | 1 | 0.59 |
| JS4451 | FTL_1393 | FTT1472c | *ppiC* | Peptidyl-prolyl *cis-trans* isomerase or parvulin | 1 | 1.05 |
| JS3773 | FTL_1404 | FTT0820 | *rplT* | 50S ribosomal protein L20 | 1 | 0.47 |
| JS3636 | FTL_1452 | FTT0773 | *rpmA* | 50S ribosomal protein L27 | 1 | 0.67 |
| JS2817 | FTL_1461 | FTT0766 | *deoD* | Purine nucleoside phosphorylase | 1 | 0.20 |
| JS2840 | FTL_1474 | FTT1314c | *greA* | Transcription elongation factor | >5 | 0.43 |
| JS1379 | FTL_1601 | FTT0463 | *yibK* | tRNA/rRNA methyltransferase | 1 | 1.00 |
| JS3633 | FTL_1912 | FTT0183c | *rpsA* | 30S ribosomal protein S1 | 1 | 0.46 |
| Substrate binding/transport | | | | | | |
| JS4252 | FTL_0133 | FTT0249 | *feoB* | Ferrous iron transport protein | 1 | 1.0 |
| JS2678 | FTL_0617 | FTT1441 | *bfr* | Bacterioferritin | 2 | 0.95 |
| JS3451 | FTL_0837 | FTT1125 | *metQ* | D-Methionine-binding transport protein | 1 | 0.68 |
| JS3166 | FTL_1233 | FTT0968c | | Amino acid antiporter | 1 | 0.69 |
| JS4295 | FTL_1458 | FTT0769 | *secA* | Preprotein translocase, subunit A | 1 | 0.83 |
| JS1673 | FTL_1528 | FTT0708 | | Major facilitator superfamily transport protein | 2 | 0.34 |
| JS4666 | FTL_1622 | FTT0444 | | Multidrug transporter | 1 | 1.06 |
| JS4221 | FTL_1672 | FTT0105c | | Transporter AcrB/AcrD/AcrF family | 1 | 0.71 |
| JS1500 | FTL_1750 | FTT0138 | *secE* | Preprotein translocase, subunit E | 1 | 0.79 |
| JS3225 | FTL_1936 | FTT0209c | | Periplasmic solute-binding family protein | 1 | 0.90 |
| JS3948 | FTL_1947 | FTT1782c | *yjjk* | ABC transporter ATP-binding protein | 2 | 0.50 |
| Others | | | | | | |
| JS4680 | FTL_0012 | FTT1750 | *recA* | Recombinase A protein | 1 | 0.83 |
| JS3972 | FTL_0337 | FTT0843 | | Unknown | 1 | 1.00 |
| JS1488 | FTL_0430 | FTT0910 | | Unknown | 4 | 0.66 |
| JS1048 | FTL_0439 | FTT0918 | | Unknown | >5 | 1.24 |
| JS3952 | FTL_0440 | FTT0920 | | Transposase | 1 | 0.95 |
| JS3638 | FTL_0514 | FTT1611 | | Unknown | 1 | 0.84 |
| JS4714 | FTL_0663 | FTT1400c | | Unknown | 1 | 0.70 |
| JS4635 | FTL_0723 | FTT1221 | | Unknown | 1 | 0.57 |
| JS3434 | FTL_0803 | FTT1152 | | Unknown | 2 | 0.78 |
| JS1020 | FTL_1075 | FTT1015 | | Unknown | 1 | 0.71 |
| JS4619 | FTL_1225 | FTT0975 | | Unknown | 1 | 0.94 |
| JS3599 | FTL_1623 | FTT0443 | | Unknown | 1 | 0.74 |
| JS2308 | FTL_1832 | FTT0029c | | Unknown | 1 | 0.61 |
| JS4698 | FTL_1867 | FTT1726 | *yegQ* | Protease | 1 | 1.06 |

[a] A single mutant for each ORF is shown when multiple independent mutants were identified for the ORF.

[b] The ORF designations are adopted from the annotations of the LVS genome (accession no. AM233362). For the genes with multiple alleles (the *iglABC* and 16S rRNA genes), the precise alleles with transposon interruption were not determined. Only one of the possible insertion sites is listed.

[c] The ORF designations are adopted from the annotations of the Schu S4 genome (accession no. NC_006570). NA indicates the absence of the LVS ORF ortholog in the Schu4 genome.

[d] The gene designations and functions are adopted from the annotated genome sequences of LVS (accession no. AM233362) and Schu S4 (accession no. NC_006570). CoA, coenzyme A.

[e] Independent mutants with insertions at different positions of each ORF.

[f] The in vitro GI was calculated based on changes in the $OD_{600}$ of each culture within the first 18 h of cultivation as described in Materials and Methods.

cloned in the NdeI site of the *E. coli-Francisella* shuttle plasmid pMP633 (44). *capB* and *capC* were inserted between the ATG start and second codon of the hygromycin resistance gene, resulting in plasmid pST1032 and pST1033. To compensate the loss of a ribosome binding site and translational start codon, a 17-bp 5′ noncoding sequence of the *F. tularensis fopA* gene (5′-GTATTTAAA GGAGTTTT-3′) was added to the reverse primers Pr1103 and Pr1104. This configuration allowed the *Francisella groEL* promoter to drive *capB* (or *capC*) and the hygromycin resistance gene. Because the hygromycin resistance gene solely relied on the added ribosome binding site at the 3′ end of the *capB* or *capC*

insert for translation, only one orientation of the cloned PCR products was identified in hygromycin-resistant *E. coli* clones. This configuration also ensured the expression of the *cap* genes due to selection for hygromycin resistance. The sequences of the complementation constructs were confirmed by DNA sequencing. pST1032 and pST1033 were electroporated into the *capB* and *capC* mutants JS2512 and JS2531, respectively, and used to infect BALB/c mice as indicated below.

**Site-specific mutagenesis in *F. tularensis*.** The *capB*, *capC*, and *capA* genes were deleted in LVS by allelic replacement and counterselection using conjugative plasmid pDMK as described elsewhere (29). pDMK also carries the Tn5
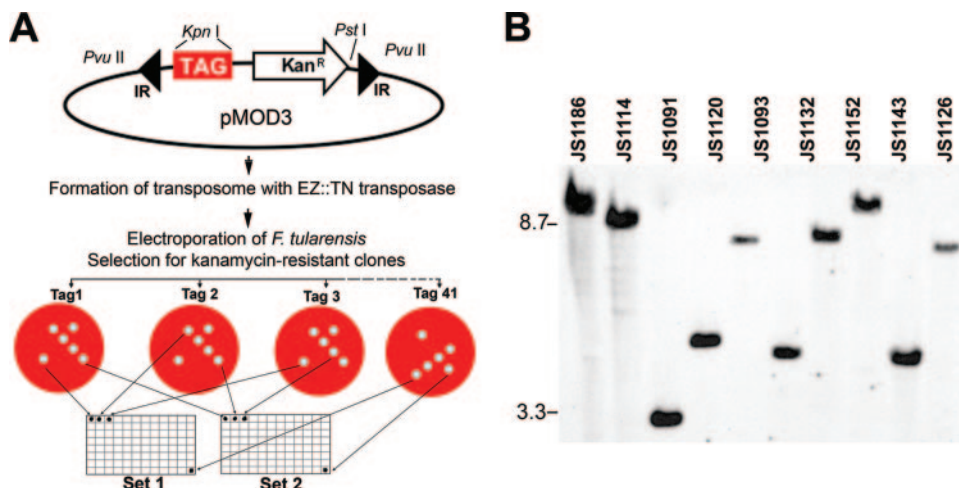
FIG. 1. Construction of STM strains in LVS by transposon mutagenesis. (A) The 52-bp oligonucleotide tags were separately cloned in the KpnI-digested EZ::TN transposon as marked by inverted repeats (IR). The tagged transposon was liberated by digestion with PvuII and mixed with EZ::TN transposase to form a transposome for transformation into LVS. The kanamycin-resistant transformants were sorted into various sets based on the sequence identity of the tag in each of the transposons. (B) Detection of transposons in STM strains. A DNA blot representing 10 STM strains was probed with a 270-bp probe representing the kanamycin resistance cassette (Kan$^r$) of the tagged transposon. The molecular sizes of DNA markers are marked in bases.

kanamycin resistance marker and the *Bacillus subtilis sacB* gene, a counterselection marker (25), and was generously provided by Anders Sjostedt. A 1.1-kb DNA fragment upstream of the *capB* gene (including the 29-bp 5′ *capB* coding region) was amplified from LVS chromosomal DNA by PCR using primers Pr890 (5′-GGCGAGCTCTTGATGGGACCTATAGGCAGTGTG-3′) and Pr891 (5′-ATCCTGAATTCAATTAACCAAAAATCCAAAGTAGTCA-3′). This 5′-flanking region was cloned into SacI- and EcoRI-digested pBluescript II SK(−) (Stratagene, La Jolla, CA) in *E. coli* DH5α, resulting in plasmid pST933. The 3′-flanking sequence, including the last 82 bp of the *capA* coding region, was amplified with primers Pr892 (5′-ATCCTGAATTCTTACTTGTTATCGATAT TAGTTTAGTAG-3′) and Pr893 (5′-CTTGTCTCGAGATCTTTGTAATGCT TTGTCAGTTT-3′). The high-fidelity DyNAzyme EXT DNA polymerase (New England Biolabs) was used for all PCR amplifications to minimize sequence errors. The 3′-flanking PCR product was cloned into the EcoRI/XhoI site of pBluescript II SK(−), resulting in plasmid pST934. To link the up- and downstream sequences, the insert DNA of pST934 was subcloned into the EcoRI/ XhoI site of pST933, and the resulting final plasmid was designated pST935. Finally, the insert sequence in pST935 was moved into SacI/XhoI-digested pDMK, resulting in the plasmid pDMK::capLVS or pST937.

pST937 was verified by DNA sequencing, transferred to *E. coli* S17-1, and used to perform conjugation with LVS as described elsewhere (29). The conjugation mixtures were first plated onto chocolate agar containing 100 μg/ml of polymyxin B for counterselection of the donor *E. coli* strain and 10 μg/ml kanamycin for selection of LVS transformants carrying the pST937 plasmid on the chromosome. To generate deletional mutants in the *capBCA* locus, the kanamycin-resistant transformants were streaked on chocolate agar plates containing 5% (wt/vol) sucrose. The sucrose-resistant colonies were further screened for the loss of kanamycin resistance. The resulting clones were examined for the *capBCA* deletion by PCR using two *capBCA*-flanking primers, Pr896 (5′-AGCTGCACC TGAGTTATTTGAT-3′) and Pr903 (5′-TCCCCTGAGCTTCTAACTTGA-3′). Correct deletion in the *capBCA* locus was further verified by DNA sequencing of the PCR products from the positive clones. Clone ST938 was selected for further characterization.

**Mouse infection with attenuated LVS mutants.** For competitive infection, the wild-type LVS and each of the attenuated mutants were separately cultured overnight in MHB, diluted to approximately $4 \times 10^5$ CFU/ml with sterile PBS, and thoroughly mixed at a 1:1 ratio. The mixtures (40 μl each, ~16,000 CFU) were used to infect groups of three BALB/c mice by intranasal inoculation as described above. Portions of the same mixtures were diluted with PBS and plated on chocolate agar plates in the presence or absence of kanamycin (10 μg/ml) to determine the actual infection doses. Only the mutants were expected to grow on the kanamycin-containing plates. The mice were sacrificed 7 days postinfection to harvest the lungs, livers, and spleens. The organs were homogenized, serially diluted with PBS, and plated on chocolate agar dishes to determine the viable

bacterial levels as described above. The level of attenuation is expressed as the competitive index (CI), which is defined as the output ratio (mutant/wild type) divided by the input ratio (mutant/wild type). The data are also expressed as the fold change of attenuation by dividing the CFU values of the recovered mutants by those of LVS.

The infection experiments with the complemented *capBC* insertion mutants and *capBCA* deletion mutant were performed in a similar manner. BALB/c mice were intranasally infected with doses as indicated in the figure legends for Fig. 3 and 4, below. Mice were sacrificed 7 days later to determine bacterial levels in the lungs, livers, and spleens as described above.

## RESULTS

**Construction of tagged mutants in *F. tularensis* strain LVS.** As illustrated in Fig. 1A, tagged mutants were generated in *F. tularensis* LVS using a derivative of the Tn5-based EZ::TN transposon (36). A series of signature-tagged transposons were generated by insertion of unique 52-bp tag sequences as described in Materials and Methods. Each of the tagged transposons was used to generate insertion mutants in LVS by electroporation as described elsewhere (36). Our Southern blot analysis of selected transposon mutants indicated that the tagged transposons inserted into the chromosome of *F. tularensis* LVS in a highly random manner (Fig. 1B). Mutants were assembled into sets of 41, each with a unique tag, for further screening in mice.

**Establishment of lung infection screening model in mice.** A key requirement for successful STM screening is the ability to recover sufficient numbers of inoculated bacteria from live animals postinfection to allow the identification of each representative mutant that survives within the mutant pool (10). To this end, it is critical to select an appropriate animal model and adequate parameters that includes infection route, dose, and duration of infection time. We initially assessed the feasibility of a mouse infection model for our STM screening. Various laboratory mouse strains have been successfully used to study respiratory infection of *F. tularensis* (20). Consistent with previous reports (18, 22), our preliminary experiments
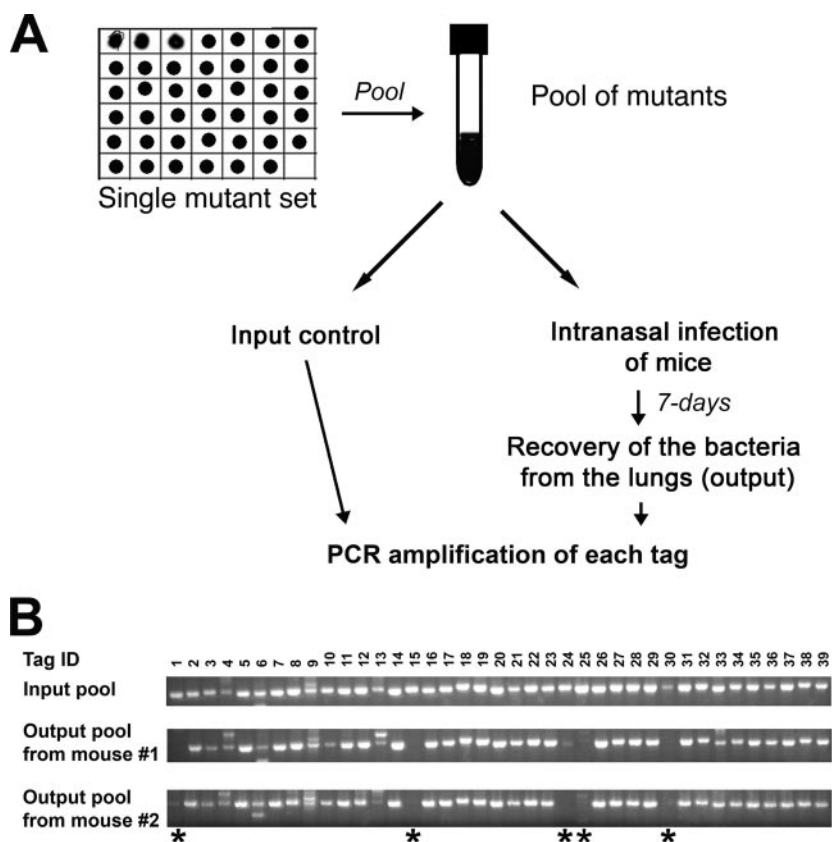
FIG. 2. Negative screening of the STM pools in mice. Each mutant in a single set was grown separately to an $OD_{600}$ of 0.35 to prepare the input mutant pool. The pool was used to infect four BALB/c mice by intranasal inoculation. The mice were sacrificed 7 days postinfection to remove the lungs and recover the bacteria (output). The input and output pools of the same mutant sets were compared by amplifying the transposon with tag-specific primers and detection by agarose gel electrophoresis. The mutants that were missing in the output pools from multiple mice infected with the same input pools are indicated with asterisks.

indicated that, among commonly used mouse strains, BALB/c mice are relatively resistant to respiratory infection with LVS. BALB/c mice were able to survive intranasal infection with $5 \times 10^3$ CFU of LVS in the first week of infection (data not shown). This resistance level allowed relatively large infection doses of the mutant pools, thereby maximizing the representation of each mutant in the pools. To test the feasibility of the BALB/c mouse model, we performed infection experiments with a pool of 41 STM strains via intranasal inoculation at various infection doses ($10^3$ to $10^4$ CFU) (Fig. 2A). At various time points following inoculation, pairs of mice were euthanized to determine the number of CFU in the lungs of each mouse. An infection dose of $5 \times 10^3$ CFU resulted in minimal mortality in the first 7 days of infection while allowing consistent recovery of all inoculated STM strains from the lungs of multiple infected mice except for those truly "attenuated" mutants (see the next section for screening procedures). These infection conditions were applied in screening the rest of the STM pools.

**Selection and screening of attenuated mutants.** A total of 96 sets of 41 mutants, totaling 3,936 strains, were screened in the BALB/c mouse model of respiratory tularemia as described above. We typically recovered thousands of bacterial colonies from the lungs of each infected mouse. In contrast, the colonies recovered from liver and spleen samples were much less numerous and were highly variable from mouse to mouse un-

der the same conditions. For these reasons, we focused our STM screening on the bacteria recovered from the lungs. When the tissue lysates yielded relatively low numbers of bacterial colonies (<500 CFU), the PCR results became inconsistent among animals infected with the same input pools (unpublished observation). We therefore repeated all infection experiments that either yielded low numbers of bacterial colonies in the output pools or the highly contaminated output colonies as assessed by colony size and morphology.

The presence or absence of individual mutants in the input and output pools was detected by PCR using tag-specific primers. This screening procedure identified 341 strains that were completely missing or substantially underrepresented in the PCR profiles, representing 8.7% of the total strains screened. These strains are referred to as attenuated mutants hereafter. The proportion of the attenuated mutants identified in this screening is within the range (5 to 15%) of previous studies with other pathogens (10). Transposon insertion sites on the chromosomes of these attenuated mutants were mapped by DNA sequencing of the genome-transposon junctions. Sequence analyses localized the transposon insertion sites in 95 LVS genes, representing 4.8% of the 1,968 predicted open reading frames (ORFs) in the LVS genome (accession no. AM233362). The identified genes have been assigned into six

TABLE 2. Confirmation of attenuation phenotypes of selected STM strains

| Mutant ID[a] | ORF disrupted | Gene[b] | In vivo CI[c] (mean + SE) | Fold attenuation[d] | Reference(s)[e] |
|---|---|---|---|---|---|
| JS1967 | FTL_0094 | *clpB* | 0.00018 + 0.00015 | 5,556 | 31, 71 |
| JS3579 | FTL_0113 | *iglC* | 0.18240 + 0.18538 | 6 | 31, 39, 63 |
| JS2788 | FTL_0439 |  | 0 | AV | |
| JS3200 | FTL_0519 | *minD* | 0.00556 + 0.00769 | 180 | 1 |
| JS1838 | FTL_0894 | *lon* | 0.00200 + 0.00191 | 500 | |
| JS4467 | FTL_0960 | *sthA* | 0 | AV | |
| JS1415 | FTL_1240 | *aroG* | 0 | AV | |
| JS4709 | FTL_1328 | *fopA* | 0.00008 + 0.00105 | 12,500 | 23, 49, 71 |
| JS4622 | FTL_1414 | *capA* | 0.00001 + 0.00001 | 100,000 | |
| JS2531 | FTL_1415 | *capC* | 0 | AV | |
| JS2512 | FTL_1416 | *capB* | 0 | AV | |
| JS2840 | FTL_1474 | *greA* | 0.00024 + 0.00015 | 4,167 | |

[a] The same representative mutant of each gene as listed in Table 1 was chosen to perform the coinfection analysis in mice.

[b] The gene designations are adopted from the annotations of the LVS and Schu S4 genomes.

[c] In vivo CI for each mutant represents the mean + standard error of the CFU values obtained from the lungs of the three mice infected with the same mutant–wild-type mixture as described in Materials and Methods.

[d] Fold attenuation represents the reciprocal of the in vivo CI. AV, only the parent strain LVS was detected in the lungs of the mice coinfected with the LVS-mutant mixture.

[e] Relevant publications for *F. tularensis* are indicated.

functional groups according to available information from experimental studies and sequence-based predictions (Table 1).

Except for FTL_1134 and FTL_0439, all of the genes identified in LVS are present in the fully sequenced genomes of other *F. tularensis* strains, including OSU18 (type B) (54) and Schu S4 (type A) (40). Some of the genes identified in this study have been previously implicated as virulence determinants of *F. tularensis* by other investigators, including *minD* (1), *clpB* (31), the intracellular growth locus (*iglA*, *iglB*, and *iglC*) (31, 39, 63), and the LPS O-antigen biosynthesis locus (*wbtA* and *wbtF*) (12, 56, 72). However, the majority of these genes represent novel bacterial factors that have not been previously associated with *F. tularensis* virulence.

To help interpret the in vivo screening results, we also determined the growth rate of the mutants that represented each of the 95 identified genes. As listed in Table 1, the in vitro growth index values for the majority of these representative mutants are around 1, thus demonstrating that the transposon insertions in the represented genes had little or no effect on the in vitro growth of the LVS derivatives. A small subset of the mutants showed various levels of growth defect as exemplified by the mutants of FTL_1328 (*fopA*), FTL_0094 (*clpB*), FTL_0891 (*tig*), and FTL_0382 (*rocE*). It is possible that the growth defects contributed to the attenuation phenotype of these mutants. Many of the identified genes were represented by multiple independent mutants with disruptions in different locations, therefore confirming the reproducibility of this STM screening.

**Verification of infection-defective status of selected mutants.** To determine the level of attenuation quantitatively, selected mutants from different functional groups were used in coinfection experiments with the wild-type strain. Each of the chosen mutants was mixed with the wild-type LVS in a 1:1 ratio and used to infect mice via intranasal inoculation. As listed in Table 2, all of the mutants tested were attenuated to various extents in terms of their ability to replicate and survive in the

lungs. Growth defects observed in vitro might have contributed to the attenuation phenotypes for some of the mutants (JS1967-*clpB*, JS1838-*lon*, JS1415-*aroG*, JS4709-*fopA*, and JS2840-*greA*). The rest of the tested mutants had no apparent in vitro growth defect. The decreased survival of these mutants in the lungs of mice was due to their defective growth in vivo and/or increased susceptibility to innate immune mechanisms of the host.

The *iglC* mutant JS3579 had the least reduction (sixfold) in the ability to survive in the lungs, whereas the mutants representing *sthA* (JS4467), *capB* (JS2512), and *capC* (JS2531) were undetectable at the end of the coinfection experiments. JS3579 carried an insertion immediately after the 162nd nucleotide of the *iglC*-coding sequence. *iglC* is the third gene in the intracellular growth locus operon (*iglABCD*), which is required for intracellular survival of *F. tularensis* (31, 39, 63). There are two copies of the *iglABCD* operon in the LVS genome as a part of the pathogenicity island (29). Since the transposon appeared to insert into one of the two *iglC* loci, the result suggests that two copies of the *iglABCD* operon are necessary for efficient growth of *F. tularensis* in vivo. Consistent with this notion, multiple mutants with insertions in *iglA* and *iglB* of the same operon were also attenuated (Table 1). Interestingly, Golovliov et al. showed that deleting one of the *iglC* genes did not affect the ability of LVS to grow in mouse J774.1 macrophages or mouse peritoneal exudate cells (29). We believe that the lack of functional IglC was responsible for the attenuation phenotype. However, it is also possible that a truncated form of IglC might act as a dominant negative protein in mutant JS3579 if the remaining 54 amino acids at its amino terminus possessed an inhibitory activity on the other wild-type IglC allele of the same chromosome.

As a part of our efforts to verify the attenuation status of the mutants identified in this STM screening, we also tested strain JS4467 in the category of metabolism and biosynthesis, because it did not show a significant in vitro growth defect (Table 1). Strain JS4467 carried a transposon disruption between nucleotides 58 and 59 in the *sthA*-coding region. *sthA* encodes an uncharacterized soluble pyridine nucleotide transhydrogenase involved in the conversion of NADPH generated by peripheral catabolic pathways to NADH, which can enter the respiratory pathway for energy production. The in vivo survival deficiency in strain JS4467 was therefore likely due to impaired energy generation.

Strain JS1967, with a transposon insertion at the 3′ region of *clpB*, showed a severe deficiency (5,556-fold reduction) in this lung infection model. Gray et al. first showed that the *clpB* gene is required for intracellular growth of *F. tularensis* subsp. *novicida* in the murine macrophage line J774.1 (31). This finding was recently confirmed by an independent mutant screening study of *F. tularensis* subsp. *novicida* with the murine macrophage line RAW (71). ClpB, a highly conserved ATP-dependent protease, participates in solubilization and refolding of aggregated proteins, especially when the organisms experience stress conditions, such as high temperatures and oxidative pressure (28). The attenuation phenotype of strain JS1967 might be caused by the impaired capability of intracellular survival and/or replication due to the lack of the ClpB chaperone function. Along the same line, strain JS1838, with a disruption immediately after the translational start

codon of *lon*, also exhibited 500-fold reduction in the capacity of in vivo growth. The Lon and Clp proteins are stress-induced ATP-dependent proteases that are responsible for removing stress-damaged proteins in bacteria (47). *lon* is the last gene in an apparent operon with *tig* (the trigger factor Tig), *clpP* (protease subunit ClpP of the ClpXP protease), and *clpX* (ATPase subunit ClpX of the ClpXP protease). While the trigger factor is involved in folding of newly synthesized proteins (17), the ClpXP protease is involved in ClpB-independent proteolysis (6). Interestingly, multiple attenuated mutants were also identified in *tig*, *clpP*, and *clpX* (Table 1), indicating that protein folding and degradation by these proteases are critical for the in vivo lifestyle of *F. tularensis*.

Mutant JS3200, with a disruption in the 3′ region of *minD*, showed a 180-fold reduction in in vivo survival. MinD is a highly conserved septum site-determining protein along with MinC and MinE. A MinD-deficient mutant of *F. tularensis* subsp. *novicida* was found to be avirulent in mice and sensitive to serum and oxidative killing (1). In *Escherichia coli*, MinD controls the site of mid-cell division by recruiting MinC and MinE to form the membrane-associated polar zone and the MinE ring (58). In agreement with this result, two independent mutants were also identified in *minC* (Table 1). *minC*, *minD*, and *minE* are organized as an apparent operon with five additional genes. These data suggest that appropriate bacterial division is essential for in vivo growth and virulence of multiple *F. tularensis* subspecies.

Strain JS4709, carrying an insertion in the 5′ region of *fopA*, was attenuated by 4 orders of magnitude in the coinfection experiments (Table 2). FopA was originally identified as a heat-modifiable protein in *F. tularensis* subsp. *novicida* (49). Tempel et al. (71) recently showed that the *fopA* mutants of *F. tularensis* subsp. *novicida* are deficient in growing in the murine macrophages. Sequence analysis suggested that *fopA* is not a part of any operon structure with its adjacent genes based on the length of the intergenic regions and the gene direction.

Finally, we confirmed the attenuation phenotype of mutant JS2840, which contained an insertion in the 3′ region of *greA*. Compared with the parent LVS strain, JS2840 was attenuated by 4,167-fold in the coinfection experiments (Table 2). GreA acts as a transcriptional elongation factor in *E. coli* by promoting the transcription of certain genes through suppressing the pausing and arrest of the RNA polymerase (5). *E. coli* cells lacking both GreA and GreB (another transcriptional elongation factor) are hypersensitive to temperature changes (52). GreA was found to be essential for *Yersinia pestis* virulence in a subcutaneously infected mouse model (21). GreA appears to be the only transcriptional elongation factor in *F. tularensis*, because an extensive search of multiple *F. tularensis* genomes did not identify a GreB homolog. *greA* appears to be a part of a multigene operon along with FTL_1477 (thiamine pyrophosphokinase), FTL_1476 or *pgi* (glucose-6-phosphate isomerase), FTL_1475 (type IV pilus fiber building block protein), and FTL_1473 or *uvrA* (DNA excision repair enzyme, subunit A of the UvrABC system). Interestingly, mutants JS4653 and JS1091 with insertions in FTL_1475 and FTL_1473, respectively, were among the attenuated strains identified in this screening (Table 1).

**Polar effect of the transposon.** A large number of the identified genes are members of apparent operon clusters, raising the possibility that the attenuation phenotypes for some of the mutants could be due to a polar effect on the downstream genes. We chose to assess this issue with the transposon insertion strains in the gene locus of FTL_1416, FTL_1415, and FTL_1414. Based on the sequence similarity of these genes to the capsule biosynthesis genes of other bacteria (see the next section), we have designated FTL_1416, FTL_1415, and FTL_1414 as *capB*, *capC*, and *capA*, respectively. As illustrated in Fig. 3, the *capBCA* genes are separated with short intergenic sequences. Our preliminary reverse transcriptase PCR analysis suggested that the *capBCA* genes are cotranscribed (unpublished observation).

We reasoned that the transposon mutants in *capB* or *capC* could not be complemented if the observed attenuation in these mutants were due to a polar effect on the downstream *capA* gene. The wild-type *capB* and *capC* were individually cloned into shuttle vector pMP633 (44). As shown in Fig. 3, in *trans* expression of the intact *capC* in the transposon mutant JS2531 (*capC*) provided significant complementation of the survival defect of the mutant in the lungs of BALB/c mice 7 days after intranasal inoculation. It should be noted that the *capB*-complemented strains JS2512 (*capB* insertion mutant) barely missed the significance cutoff ($P < 0.05$) due to a large intergroup variation in the mice infected with this strain, but the trend was similar to that of the *capC*-complemented mutant JS2531. These findings show that the observed attenuation phenotypes with the *capB* and *capC* insertion mutants were at least in part due to mutations in *capB* and *capC*. Thus, the complementation experiments suggest that the transposon may not block transcriptional read-through into the downstream genes. It should be noted that, in both of the complemented strains, the values were still over 10-fold less than the wild-type value. These differences could be caused by multiple possibilities, such as instability of the shuttle plasmid during infection, inappropriate in *trans* expression levels of the CapB and CapC proteins, and a partial polar effect.

**Requirement of the putative capsule genes for infection.** Among the attenuated strains are those with disruptions in the putative capsule biosynthetic *capBCA* genes (Table 1). At the amino acid level, FTL_1416 and FTL_1415 share 38% and 29% sequence homology with the CapB and CapC of *Bacillus anthracis*, respectively. CapB and CapC, together with CapA, CapD, and CapE in *B. anthracis*, are responsible for the biosynthesis of the capsule. Unlike common polysaccharide-based capsules in the vast majority of bacterial species, the *B. anthracis* capsule is composed of poly-γ-D-glutamic acids (PGA) (8). The PGA-based capsule in *B. anthracis* is a major virulence factor due to its antiphagocytic property (38).

In *B. anthracis*, CapB and CapC are believed to form a tight membrane-associated complex to catalyze the synthesis of PGA (4), whereas CapA is suggested to be a transporter (3). We named FTL_1414 CapA based on its predicted transporter function as a putative transmembrane protein, although FTL_1414 does not resemble any of the *B. anthracis* capsule genes. CapD, γ-glutamyltranspeptidase, is required for the covalent attachment of the *B. anthracis* capsule to the cell wall peptidoglycan (7). An ortholog of the *B. anthracis* CapD exists elsewhere in the *F. tularensis* LVS genome (FTL_0766), although this screening did not identify a *capD* mutant.

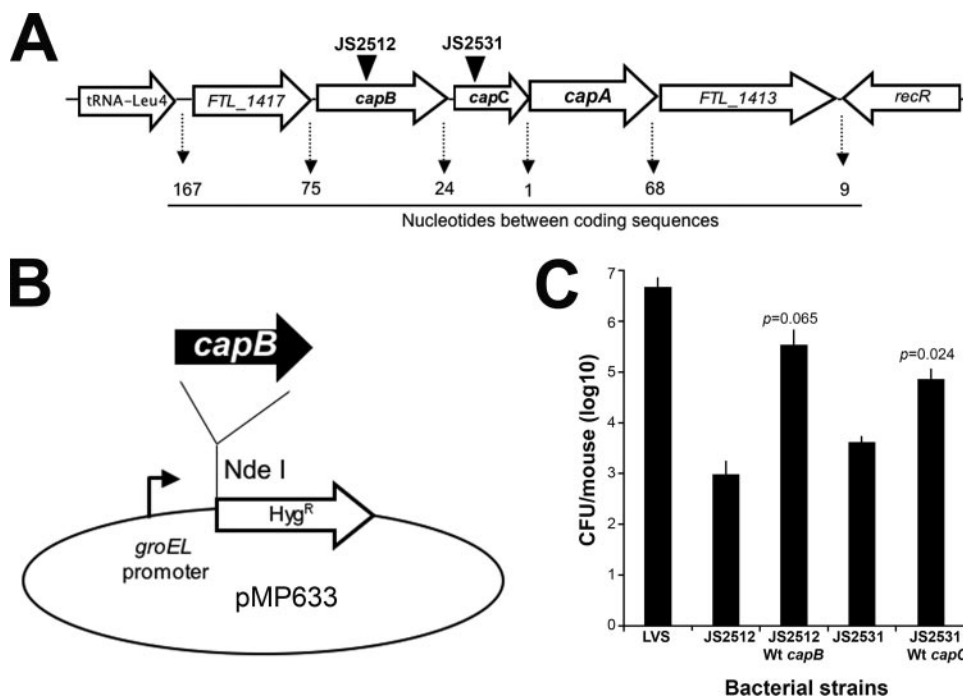The PGA-based capsule has been identified in only a few

FIG. 3. In *trans* complementation of the *capB* and *capC* disruptive mutants. (A) Genetic organization of the *capBCA* locus in LVS. The genes and their coding directions are represented with open arrows and arrowheads, respectively. The transposon insertion sites of the *capB* (JS2512) and *capC* (JS2531) mutants are indicated with vertical arrowheads. The numbers of intergenic nucleotides are indicated at the bottom. (B) Generation of complementation constructs in plasmid pMP633. The wild-type *capB* and *capC* genes of LVS were inserted into the NdeI site of pMP633. (C) Bacterial load in lungs of mice infected with LVS and isogenic transposon mutants. BALB/c mice were intranasally infected with strains LVS (12,400 CFU/mouse), JS2512 (*capB* mutant; 30,840 CFU/mouse), JS2531 (*capC* mutant; 28,000 CFU/mouse), *capB*-complemented JS2512 (34,000 CFU/mouse), and *capC*-complemented JS2531 (30,000 CFU/mouse). The bars represent the mean CFU values + standard errors of bacterial levels in the lungs of three mice 7 days postinfection. *P* values were determined based on comparisons of the values between the transposon mutants and corresponding in *trans*-complemented strains using Student's *t* test in Microsoft Excel.

gram-positive bacteria, such as *B. anthracis* and *Staphylococcus epidermidis* (37). However, recent genome sequencing studies have also revealed orthologs for PGA biosynthesis genes in several other gram-negative bacteria, including *Idiomarina baltica* (35), *Rhodopirellula baltica* (27), *Leptospira interrogans* (57), *Oceanobacillus iheyensis* (68), and *Desulfitobacterium hafniense* (51). It is intriguing that these bacteria, along with *F. tularensis*, are all associated with water environments. As represented in Fig. 3, the *capBCA* genes of *F. tularensis* are also similar to the putative PGA biosynthetic genes in these bacteria (Fig. 3). The *capBCA* and *capD* genes found in LVS are also conserved in other *F. tularensis* strains, including OSU18 (accession no. CP000437) (54) and Schu S4 (accession no. AJ749949) (40).

We confirmed the attenuation of the mutants with disruptions in the *capBCA* locus by coinfection experiments. As shown in Table 2, the representative transposon mutants in *capB* (strain JS2512), *capC* (strain JS2531), and *capA* (strain JS4622) were out-competed by the parent strain in the lung infection model. The *capB* and *capC* mutants (JS2512 and JS2531) were completely undetectable in all three infected mice 7 days postinfection; the *capA* mutant (JS4622) was detectable in two of the three infected mice. These mutants were also compared with the parent strain LVS by separately infecting mice with individual mutants. Seven days post-intranasal inoculation, the mice infected with strain JS2512 (*capB*),

JS2531 (*capC*), or JS4622 (*capA*) had a >1,000-fold reduction in the bacterial burden in the lungs compared with those infected with LVS (data not shown).

To exclude the possibility that the attenuation of these transposon mutants was due to possible transposon insertions elsewhere in the LVS genome, we constructed deletion mutants in the *capBCA* locus. The coding sequences of the *capBCA* genes were deleted by allelic replacement as illustrated in Fig. 4. The deletion mutants were characterized by PCR amplification of the *capBCA* locus using the flanking sequence-based primers and DNA sequencing. As a result, the entire coding sequences of *capB*, *capC*, and *capA* except for the 5′ *capB* (29-bp) and 3′ *capA* (82-bp) regions were deleted in frame from the LVS chromosome by unmarked deletion. While the wild-type strain LVS showed a 3.4-kb PCR product, ST938, one of the confirmed *capBCA* deletion mutants yielded a PCR fragment with an expected size of 643 bp (Fig. 4A) and correct sequence (data not shown). Consistent with the transposon insertion mutants in the *capBCA* locus (Table 1), ST938 did not show a significant growth defect in MHB (Fig. 4B). We also wanted to generate an in *trans* complementation construct with the entire *capBCA* operon. All attempts with different shuttle plasmids yielded either partial or no inserts, suggesting that *capBCA* expression in *E. coli* may be toxic.

We compared ST938 with LVS in terms of their in vivo survival in mice. Consistent with the results obtained with
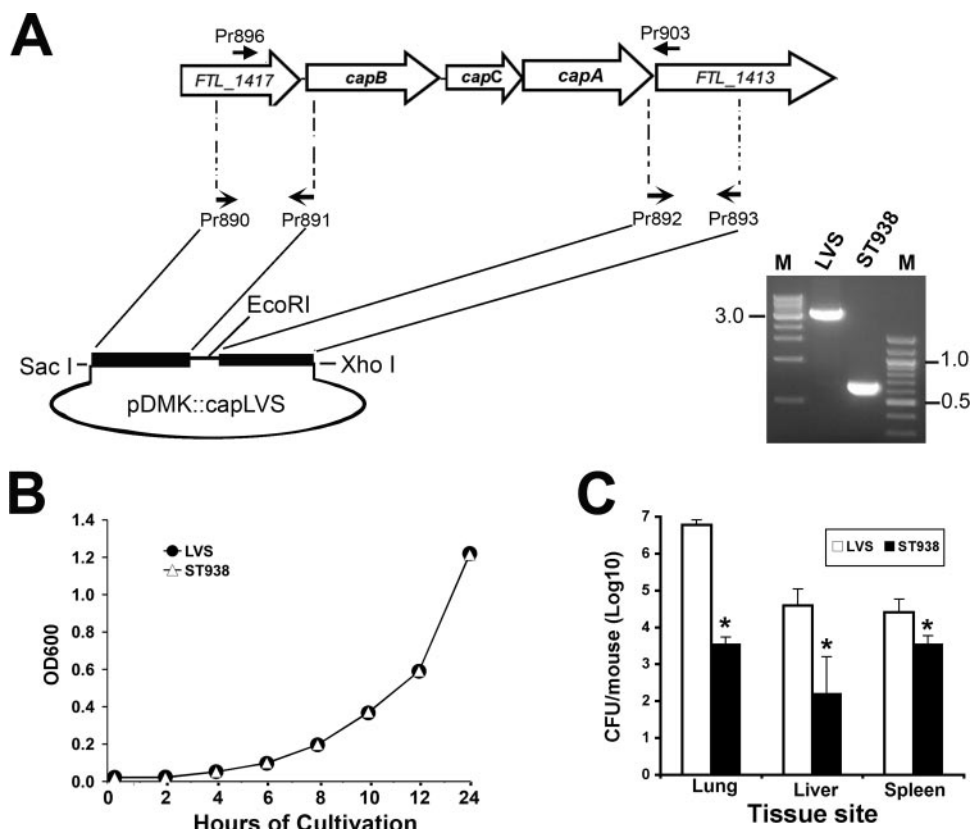
FIG. 4. Construction and characterization of the *capBCA* deletion mutant. (A) Construction of the deletional mutation in the *capBCA* locus. The sequences flanking the *capBCA* genes were separately amplified and cloned in the SacI/XhoI-digested pDMK plasmid. The resulting plasmid was introduced into LVS by conjugation. Following sequential selection steps with kanamycin and sucrose, the resultant strains (as represented by strain ST938) were examined for loss of the *capBCA* genes by PCR. The sizes of the representative molecular markers (M) are indicated in kb. Approximate locations of the relevant primers are marked with small lateral arrows. (B) Growth of the *capBCA* deletion mutant in MHB. LVS and ST938 were separately cultured in 5 ml MHB. Optical absorbance levels ($OD_{600}$) were determined for each culture at the indicated time points. The value represents the means + standard errors of five independent cultures. (C) Bacterial load in mice infected with the *capBCA* deletion mutant ST938 (6,500 CFU/mouse) and LVS (4,000 CFU/mouse). BALB/c mice were intranasally infected with ST938 or LVS and sacrificed 7 days later to determine bacterial levels in the lungs, livers, and spleens. The bars represent the mean CFU values + standard errors of six mice. Asterisks indicate P < 0.05 as determined using Student's *t* test in Microsoft Excel.

multiple transposon mutants in the *capBCA* locus (Table 2), the bacterial load in the lungs of the ST938-infected mice was 1,697-fold lower than the mean CFU value obtained with the LVS-infected mice 7 days postinfection (Fig. 4C). The *capBCA* mutant strain also showed significantly reduced levels of overall bacterial burden in other tissue sites. When compared with the LVS-infected mice, the bacterial loads in the livers and spleens of the ST938-infected mice were decreased by 241- and 7.3-fold, respectively (Fig. 4C). Finally, all 12 mice infected with ST938 survived throughout the 3-week infection experiments, whereas all of the mice infected with a similar dose of LVS died in the first 2 weeks postinfection (data not shown). These results demonstrate that the *capBCA* locus is critical for in vivo replication/survival and virulence of *F. tularensis*.

## DISCUSSION

This study represents the first extensive search of *F. tularensis* virulence determinants by completing an STM study in a respiratory infection mouse model. We have identified a total of 95 genes required for the survival of LVS in the lungs of mice. All but 2 of the 95 genes identified in LVS are present in the fully sequenced genomes of other *F. tularensis* strains, including OSU18 (54) and Schu S4 (40). It is thus reasonable to expect that at least some of the factors identified in this study, if not all, are important for the pathogenic process of fully virulent *F. tularensis* strains. The majority of the genes identified in this study, including the *capBCA* locus, are also present in the recently released genome of *F. tularensis* subsp. *novicida* strain U112 (GenBank accession no. CP000439). Strain U112 has been commonly used to identify most of the known *F. tularensis* virulence factors, including the intracellular growth *iglABCD* locus (24, 31, 42, 71). These findings are consistent with the highly conserved genetic contents among various *F. tularensis* subspecies as revealed by recent genomic studies (40, 54). Our findings along with other studies argue that the genetic basis of *F. tularensis* adaptation and virulence is highly similar among different subspecies; it is perhaps the minor genetic variations and/or epigenetic differences among different *F. tularensis* subspecies and strains that determine the outcome of infection in various mammalian hosts. This inves-

tigation has greatly expanded current knowledge regarding the genetic basis of *F. tularensis* virulence.

Some of the genes identified in this study have been previously implicated as virulence determinants of *F. tularensis* by other investigators. Included among those are MinD (1), ClpB (31, 71), the intracellular growth locus (31, 39, 63), and the LPS O-antigen biosynthesis locus (12, 56, 72). This study has also revealed a large list of novel *F. tularensis* genes that are required for in vivo survival. Consistent with previous STM studies in other pathogens (10), this STM analysis has identified a number of genes that are involved in basic metabolism and physiology. Impaired growth in vivo might be the cause for the attenuation of some mutants in this category. In a strict sense, the genes involved in basic metabolism and physiology should not be regarded as virulence factors (9). However, the information along this line can be valuable for treatment and prevention of tularemia. The metabolic genes identified in this study may be targeted for future development of therapeutic agents. In particular, the attenuated strains of metabolic genes can be used to develop genetically defined vaccines against virulent *F. tularensis* strains.

A significant number of the genes identified in this study have apparent functions in intracellular growth/survival of the bacterium. Besides the intracellular growth locus (*iglABCD*), the identified proteases/chaperones (ClpB, ClpXP, Lon, and Tig) are particularly interesting in the context of in vivo adaptation of *F. tularensis* to various stress conditions. These conserved proteins are required for protein folding and/or degradation in many bacteria (6, 30). Recent studies have demonstrated that *F. tularensis* is able to survive in the phagosomes of macrophages and replicate in cytoplasm (62). It is reasonable to believe that these proteases/chaperones may promote the survival and replication of *F. tularensis* in mammalian hosts by refolding misfolded proteins and removing the damaged proteins or normal proteins that become unnecessary or detrimental to the bacterium under certain stress conditions. Mpa, a Clp-like protease in the proteasome of *Mycobacterium tuberculosis*, has been demonstrated to be necessary for bacterial resistance to nitric oxide and growth in macrophages (14, 15). Identification of attenuated mutants with insertions in the genes encoding catalase (*katG*), DNA repair enzyme (*uvrA*), and cold shock protein (*deaD*) further supports the notion that stress-relieving mechanisms are critical for *F. tularensis* adaptation in mammalian hosts. Our data now provide specific genetic targets for further understanding of the molecular basis of *F. tularensis* adaptation in different host niches and various stages of infection.

Many attenuated mutants carried transposon insertions in the genes associated with bacterial cell surface structures (e.g., membrane proteins, LPS, and capsule). The genes in this category are particularly interesting because the encoded products may be involved in pathogen-host interactions and may also represent potential targets for future development of therapeutics and subunit vaccines. A subset of the mutants contained insertions in the genes encoding putative lipoproteins, outer membrane proteins, and transmembrane proteins. Except for FopA (FTL_1328) and Tul4 (FTL_0421), none of these proteins has been previously described. FopA, a heat-modifiable outer membrane-associated protein (49), is required for the growth of *F. tularensis* subsp. *novicida* in murine

macrophages (71). Tul4 was originally identified as a 17-kDa T-cell-stimulating lipoprotein in LVS (65, 66). A recent Tn*phoA* screening study identified six exported *F. tularensis* proteins (26), but these proteins do not match any of the putative membrane proteins identified in this study. This screening also identified *wbtA* (FTL_0592) and *wbtF* (FTL_0597), two genes encoding enzymes for modifying the LPS O-antigen. Consistent with our finding, other studies have implicated LPS as an essential surface structure for *F. tularensis* immune evasion and serum resistance (12, 32, 56, 70, 72).

We have identified a putative capsule locus in LVS which partially resembles the well-characterized capsule biosynthetic genes in *B. anthracis*. Bacterial capsules, the outermost structure of the bacterial surfaces, can provide a selective advantage by preventing desiccation in the environment and, for pathogens, by promoting adherence and conferring resistance to host defense mechanisms, such as complement-mediated phagocytosis and killing. The pXO2 plasmid-encoded *B. anthracis* capsule is a key antiphagocytic virulence factor (38). A capsule has been revealed for fully virulent *F. tularensis* strains by electron microscopy, although it is readily removed upon hypertonic treatment or aerosolization (34, 60, 67). The capsule is a key virulence factor based on the observations that unencapsulated bacteria are more susceptible to complement-mediated killing (60) and are avirulent (34). The capsule appears to contain large amounts of lipid, but other components are unknown (34). The sequence similarity between the *F. tularensis capBCA* genes and the capsular biosynthesis genes of other bacteria suggests the production of PGA in *F. tularensis*. The mouse infection experiments with various mutants of the *capBCA* locus consistently demonstrated that these genes are essential for in vivo survival and virulence of *F. tularensis*. A PGA-based capsule has only been reported in gram-positive bacteria (*Bacillus* and *Staphylococcus* species), although sequence information has suggested that PGA is produced in multiple gram-negative species (8). The identification of the *capBCA* locus as a virulence determinant of *F. tularensis* has provided ample reason for further characterization of this locus. Future characterization of the *F. tularensis capBCA* locus will also be instrumental for determining whether PGA is a constituent of the capsule in gram-negative bacteria.

All but two genetic loci identified in LVS are conserved in the other *F. tularensis* strains, OSU18 and Schu S4, in terms of predicted amino acid sequence and the local gene order. Our study has thus provided a genetic basis for further characterization of the pathogenic mechanisms of *F. tularensis* strains that are fully virulent for humans. FTL_1134 and FTL_0439 represent two LVS-specific genetic loci identified in this screening. FTL_1134, a hypothetical membrane protein, is entirely absent in the Schu S4 genome. FTL_0439 represents a fusion product of two Schu S4 genes (FTT0918 and FTT0919). A previous study showed that mutations in FTT0918 abolished the virulence of strain Schu S4 in mice (73). It is possible that FTL_0439 and FTT0918 share a common function in terms of enhancing in vivo survival of *F. tularensis*. A significant number of the *F. tularensis* genes represented by the attenuated mutants cannot be matched with apparent function. Among these are *F. tularensis*-specific genes and the genes with uncharacterized orthologs in other bacteria. Future characterization of

these "unknown" genes may be fruitful in terms of understanding the pathogenic mechanisms that are unique to *F. tularensis*.

After our STM screening was completed, other investigators observed that the promoter driving the kanamycin resistance gene in the EZ::TN transposon is inactive in *F. tularensis* (24, 46). This implies that the recovery of the *F. tularensis* transposon mutants under in vitro culture conditions requires active transcription of the target genes. Consistent with this, reexamination of our sequence data for the attenuated STM strains revealed that the kanamycin resistance gene was always orientated in the same direction as the target genes in the LVS chromosome. On one hand, these lines of information have highlighted the limitations of our mutagenesis approach in identifying virulence determinants. It is thus clear that our STM screening has missed those virulence-associated genes whose promoter activities did not support the kanamycin resistance. On the other hand, the information from this unintended "bias" has provided some important information on the biology of *F. tularensis*. Our data indicate that the *F. tularensis* genes identified in this study are actively expressed under both in vitro and in vivo conditions. There is a shortage of well-characterized promoter elements that can drive gene expression in *F. tularensis* under various conditions. We have thus provided many *F. tularensis* promoters that can drive gene expression in *F. tularensis* under culture and infection conditions.

## ACKNOWLEDGMENTS

## REFERENCES

1. **Anthony, L. S., S. C. Cowley, K. E. Mdluli, and F. E. Nano.** 1994. Isolation of a *Francisella tularensis* mutant that is sensitive to serum and oxidative killing and is avirulent in mice: correlation with the loss of MinD homologue expression. FEMS Microbiol. Lett. **124:**157–165.
2. **Anthony, L. S., and P. A. Kongshavn.** 1987. Experimental murine tularemia caused by *Francisella tularensis*, live vaccine strain: a model of acquired cellular resistance. Microb. Pathog. **2:**3–14.
3. **Ashiuchi, M., C. Nawa, T. Kamei, J. J. Song, S. P. Hong, M. H. Sung, K. Soda, and H. Misono.** 2001. Physiological and biochemical characteristics of poly gamma-glutamate synthetase complex of *Bacillus subtilis*. Eur. J. Biochem. **268:**5321–5328.
4. **Ashiuchi, M., K. Soda, and H. Misono.** 1999. A poly-γ-glutamate synthetic system of Bacillus subtilis IFO 3336: gene cloning and biochemical analysis of poly-γ-glutamate produced by *Escherichia coli* clone cells. Biochem. Biophys. Res. Commun. **263:**6–12.
5. **Borukhov, S., J. Lee, and O. Laptenko.** 2005. Bacterial transcription elongation factors: new insights into molecular mechanism of action. Mol. Microbiol. **55:**1315–1324.
6. **Butler, S. M., R. A. Festa, M. J. Pearce, and K. H. Darwin.** 2006. Self-compartmentalized bacterial proteases and pathogenesis. Mol. Microbiol. **60:**553–562.
7. **Candela, T., and A. Fouet.** 2005. Bacillus anthracis CapD, belonging to the γ-glutamyltranspeptidase family, is required for the covalent anchoring of capsule to peptidoglycan. Mol. Microbiol. **57:**717–726.
8. **Candela, T., and A. Fouet.** 2006. Poly-gamma-glutamate in bacteria. Mol. Microbiol. **60:**1091–1098.
9. **Casadevall, A., and L. A. Pirofski.** 1999. Host-pathogen interactions: redefining the basic concepts of virulence and pathogenicity. Infect. Immun. **67:**3703–3713.
10. **Chiang, S. L., J. J. Mekalanos, and D. W. Holden.** 1999. In vivo genetic analysis of bacterial virulence. Annu. Rev. Microbiol. **53:**129–154.
11. **Christenson, B.** 1984. An outbreak of tularemia in the northern part of central Sweden. Scand. J. Infect. Dis. **16:**285–290.
12. **Cowley, S. C., C. J. Gray, and F. E. Nano.** 2000. Isolation and characterization of *Francisella novicida* mutants defective in lipopolysaccharide biosynthesis. FEMS. Microbiol. Lett. **182:**63–67.
13. **Dahlstrand, S., O. Ringertz, and B. Zetterberg.** 1971. Airborne tularemia in Sweden. Scand. J. Infect. Dis. **3:**7–16.
14. **Darwin, K. H., S. Ehrt, J. C. Gutierrez-Ramos, N. Weich, and C. F. Nathan.** 2003. The proteasome of *Mycobacterium tuberculosis* is required for resistance to nitric oxide. Science **302:**1963–1966.
15. **Darwin, K. H., G. Lin, Z. Chen, H. Li, and C. F. Nathan.** 2005. Characterization of a *Mycobacterium tuberculosis* proteasomal ATPase homologue. Mol. Microbiol. **55:**561–571.
16. **Dennis, D. T., T. V. Inglesby, D. A. Henderson, J. G. Bartlett, M. S. Ascher, E. Eitzen, A. D. Fine, A. M. Friedlander, J. Hauer, M. Layton, S. R. Lillibridge, J. E. McDade, M. T. Osterholm, T. O'Toole, G. Parker, T. M. Perl, P. K. Russell, and K. Tonat.** 2001. Tularemia as a biological weapon: medical and public health management. JAMA **285:**2763–2773.
17. **Deuerling, E., H. Patzelt, S. Vorderwulbecke, T. Rauch, G. Kramer, E. Schaffitzel, A. Mogk, A. Schulze-Specking, H. Langen, and B. Bukau.** 2003. Trigger factor and DnaK possess overlapping substrate pools and binding specificities. Mol. Microbiol. **47:**1317–1328.
18. **Duckett, N. S., S. Olmos, D. M. Durrant, and D. W. Metzger.** 2005. Intranasal interleukin-12 treatment for protection against respiratory infection with the *Francisella tularensis* live vaccine strain. Infect. Immun. **73:**2306–2311.
19. **Eigelsbach, H. T., and C. M. Downs.** 1961. Prophylactic effectiveness of live and killed tularemia vaccines. I. Production of vaccine and evaluation in the white mouse and guinea pig. J. Immunol. **87:**415–425.
20. **Ellis, J., P. C. Oyston, M. Green, and R. W. Titball.** 2002. Tularemia. Clin. Microbiol. Rev. **15:**631–646.
21. **Flashner, Y., E. Mamroud, A. Tidhar, R. Ber, M. Aftalion, D. Gur, S. Lazar, A. Zvi, T. Bino, N. Ariel, B. Velan, A. Shafferman, and S. Cohen.** 2004. Generation of *Yersinia pestis* attenuated strains by signature-tagged mutagenesis in search of novel vaccine candidates. Infect. Immun. **72:**908–915.
22. **Fortier, A. H., M. V. Slayter, R. Ziemba, M. S. Meltzer, and C. A. Nacy.** 1991. Live vaccine strain of *Francisella tularensis*: infection and immunity in mice. Infect. Immun. **59:**2922–2928.
23. **Fulop, M., R. Manchee, and R. Titball.** 1995. Role of lipopolysaccharide and a major outer membrane protein from *Francisella tularensis* in the induction of immunity against tularemia. Vaccine **13:**1220–1225.
24. **Gallagher, L. A., E. Ramage, M. A. Jacobs, R. Kaul, M. Brittnacher, and C. Manoil.** 2007. A comprehensive transposon mutant library of Francisella novicida, a bioweapon surrogate. Proc. Natl. Acad. Sci. USA. **104:**1009–1014.
25. **Gay, P., D. Le Coq, M. Steinmetz, T. Berkelman, and C. I. Kado.** 1985. Positive selection procedure for entrapment of insertion sequence elements in gram-negative bacteria. J. Bacteriol. **164:**918–921.
26. **Gilmore, R. D., Jr., R. M. Bacon, S. L. Sviat, J. M. Petersen, and S. W. Bearden.** 2004. Identification of *Francisella tularensis* genes encoding exported membrane-associated proteins using Tn*phoA* mutagenesis of a genomic library. Microb. Pathog. **37:**205–213.
27. **Glockner, F. O., M. Kube, M. Bauer, H. Teeling, T. Lombardot, W. Ludwig, D. Gade, A. Beck, K. Borzym, K. Heitmann, R. Rabus, H. Schlesner, R. Amann, and R. Reinhardt.** 2003. Complete genome sequence of the marine planctomycete *Pirellula* sp. strain 1. Proc. Natl. Acad. Sci. USA. **100:**8298–8303.
28. **Goloubinoff, P., A. Mogk, A. P. Zvi, T. Tomoyasu, and B. Bukau.** 1999. Sequential mechanism of solubilization and refolding of stable protein aggregates by a bichaperone network. Proc. Natl. Acad. Sci. USA. **96:**13732–13737.
29. **Golovliov, I., A. Sjostedt, A. Mokrievich, and V. Pavlov.** 2003. A method for allelic replacement in *Francisella tularensis*. FEMS. Microbiol. Lett. **222:**273–280.
30. **Gottesman, S.** 2003. Proteolysis in bacterial regulatory circuits. Annu. Rev. Cell Dev. Biol. **19:**565–587.
31. **Gray, C. G., S. C. Cowley, K. K. Cheung, and F. E. Nano.** 2002. The identification of five genetic loci of *Francisella novicida* associated with intracellular growth. FEMS. Microbiol. Lett. **215:**53–56.
32. **Hajjar, A. M., M. D. Harvey, S. A. Shaffer, D. R. Goodlett, A. Sjostedt, H. Edebro, M. Forsman, M. Bystrom, M. Pelletier, C. B. Wilson, S. I. Miller, S. J. Skerrett, and R. K. Ernst.** 2006. Lack of in vitro and in vivo recognition of *Francisella tularensis* subspecies lipopolysaccharide by Toll-like receptors. Infect. Immun. **74:**6730–6738.
33. **Hensel, M., J. E. Shea, C. Gleeson, M. D. Jones, E. Dalton, and D. W. Holden.** 1995. Simultaneous identification of bacterial virulence genes by negative selection. Science **269:**400–403.

34. **Hood, A. M.** 1977. Virulence factors of *Francisella tularensis*. J. Hyg. (London) **79:**47–60.

35. **Hou, S., J. H. Saw, K. S. Lee, T. A. Freitas, C. Belisle, Y. Kawarabayasi, S. P. Donachie, A. Pikina, M. Y. Galperin, E. V. Koonin, K. S. Makarova, M. V. Omelchenko, A. Sorokin, Y. I. Wolf, Q. X. Li, Y. S. Keum, S. Campbell, J. Denery, S.-I. Aizawa, S. Shibata, A. Malahoff, and M. Alam.** 2004. Genome sequence of the deep-sea γ-proteobacterium *Idiomarina loihiensis* reveals amino acid fermentation as a source of carbon and energy. Proc. Natl. Aca Sci. USA. **101:**18036–18041.

36. **Kawula, T. H., J. D. Hall, J. R. Fuller, and R. R. Craven.** 2004. Use of transposon-transposase complexes to create stable insertion mutant strains of *Francisella tularensis* LVS. Appl. Environ. Microbiol. **70:**6901–6904.

37. **Kocianova, S., C. Vuong, Y. Yao, J. M. Voyich, E. R. Fischer, F. R. DeLeo, and M. E. Otto.** 2005. Key role of poly-γ-DL-glutamic acid in immune evasion and virulence of Staphylococcus epidermidis. J. Clin. Investig. **115:**688–694.

38. **Koehler, T. M.** 2002. Bacillus anthracis genetics and virulence gene regulation. Curr. Top. Microbiol. Immunol. **271:**143–164.

39. **Lai, X. H., I. Golovliov, and A. Sjostedt.** 2004. Expression of IglC is necessary for intracellular growth and induction of apoptosis in murine macrophages by *Francisella tularensis*. Microb. Pathog **37:**225–230.

40. **Larsson, P., P. C. Oyston, P. Chain, M. C. Chu, M. Duffield, H. H. Fuxelius, E. Garcia, G. Halltorp, D. Johansson, K. E. Isherwood, P. D. Karp, E. Larsson, Y. Liu, S. Michell, J. Prior, R. Prior, S. Malfatti, A. Sjostedt, K. Svensson, N. Thompson, L. Vergez, J. K. Wagg, B. W. Wren, L. E. Lindler, S. G. Andersson, M. Forsman, and R. W. Titball.** 2005. The complete genome sequence of *Francisella tularensis*, the causative agent of tularemia. Nat. Genet. **37:**153–159.

41. **Lau, G. W., S. Haataja, M. Lonetto, S. E. Kensit, A. Marra, A. P. Bryant, D. McDevitt, D. A. Morrison, and D. W. Holden.** 2001. A functional genomic analysis of type 3 *Streptococcus pneumoniae* virulence. Mol. Microbiol. **40:**555–571.

42. **Lauriano, C. M., J. R. Barker, S. S. Yoon, F. E. Nano, B. P. Arulanandam, D. J. Hassett, and K. E. Klose.** 2004. MglA regulates transcription of virulence factors necessary for *Francisella tularensis* intraamoebae and intramacrophage survival. Proc. Natl. Acad. Sci. USA. **101:**4246–4249.

43. **Lehoux, D. E., F. Sanschagrin, and R. C. Levesque.** 2002. Identification of in vivo essential genes from *Pseudomonas aeruginosa* by PCR-based signature-tagged mutagenesis. FEMS Microbiol. Lett. **210:**73–80.

44. **LoVullo, E. D., L. A. Sherrill, L. L. Perez, and M. S. Pavelka, Jr.** 2006. Genetic tools for highly pathogenic Francisella tularensis subsp. tularensis. Microbiology **152:**3425–3435.

45. **Lu, L., Y. Ma, and J. R. Zhang.** 2006. *Streptococcus pneumoniae* recruits complement factor H through the amino terminus of CbpA. J. Biol. Chem. **281:**15464–15474.

46. **Maier, T. M., R. Pechous, M. Casey, T. C. Zahrt, and D. W. Frank.** 2006. In vivo Himar1-based transposon mutagenesis of *Francisella tularensis*. Appl. Environ. Microbiol. **72:**1878–1885.

47. **Maurizi, M. R.** 1992 Proteases and protein degradation in Escherichia coli. Experientia **48:**178–201.

48. **McCrumb, F. R.** 1961. Aerosol infection if man with *Pasteurella tularensis*. Bacteriol. Rev. **25:**262–267.

49. **Nano, F. E.** 1988. Identification of a heat-modifiable protein of *Francisella tularensis* and molecular cloning of the encoding gene. Microb. Pathog. **5:**109–119.

50. **Nano, F. E., N. Zhang, S. C. Cowley, K. E. Klose, K. K. Cheung, M. J. Roberts, J. S. Ludu, G. W. Letendre, A. I. Meierovics, G. Stephens, and L. E. Elkins.** 2004. A *Francisella tularensis* pathogenicity island required for intramacrophage growth. J. Bacteriol. **186:**6430–6436.

51. **Nonaka, H., G. Keresztes, Y. Shinoda, Y. Ikenaga, M. Abe, K. Naito, K. Inatomi, K. Furukawa, M. Inui, and H. Yukawa.** 2006. Complete genome sequence of the dehalorespiring bacterium *Desulfitobacterium hafniense* Y51 and comparison with *Dehalococcoides ethenogenes* 195. J. Bacteriol. **188:**2262–2274.

52. **Orlova, M., J. Newlands, A. Das, A. Goldfarb, and S. Borukhov.** 1995. Intrinsic transcript cleavage activity of RNA polymerase. Proc. Natl. Acad. Sci. USA. **92:**4596–4600.

53. **Oyston, P. C., A. Sjostedt, and R. W. Titball.** 2004. Tularaemia: bioterrorism defence renews interest in *Francisella tularensis*. Nat. Rev. Microbiol. **2:**967–978.

54. **Petrosino, J. F., Q. Xiang, S. E. Karpathy, H. Jiang, S. Yerrapragada, Y. Liu, J. Gioia, L. Hemphill, A. Gonzalez, T. M. Raghavan, A. Uzman, G. E. Fox, S. Highlander, M. Reichard, R. J. Morton, K. D. Clinkenbeard, and G. M. Weinstock.** 2006. Chromosome rearrangement and diversification of *Francisella tularensis* revealed by the type B (OSU18) genome sequence. J. Bacteriol. **188:**6977–6985.

55. **Qimron, U., N. Madar, R. Ascarelli-Goell, M. Elgrably-Weiss, S. Altuvia, and A. Porgador.** 2003. Reliable determination of transposon insertion site in prokaryotes by direct sequencing. J. Microbiol. Methods **54:**137–140.

56. **Raynaud, C., K. L. Meibom, M. A. Lety, I. Dubail, T. Candela, E. Frapy, and A. Charbit.** 2007. Role of the *wbt* locus of *Francisella tularensis*: role in lipopolysaccharide O-antigen biogenesis and pathogenicity. Infect. Immun. **75:**536–541.

57. **Ren, S. X., G. Fu, X. G. Jiang, R. Zeng, Y. G. Miao, H. Xu, Y. X. Zhang, H. Xiong, G. Lu, L. F. Lu, H. Q. Jiang, J. Jia, Y. F. Tu, J. X. Jiang, W. Y. Gu, Y. Q. Zhang, Z. Cai, H. H. Sheng, H. F. Yin, Y. Zhang, G. F. Zhu, M. Wan, H. L. Huang, Z. Qian, S. Y. Wang, W. Ma, Z. J. Yao, Y. Shen, B. Q. Qiang, Q. C. Xia, X. K. Guo, A. Danchin, I. Saint Girons, R. L. Somerville, Y. M. Wen, M. H. Shi, Z. Chen, J. G. Xu, and G. P. Zhao.** 2003. Unique physiological and pathogenic features of *Leptospira interrogans* revealed by whole-genome sequencing. Nature **422:**888–893.

58. **Rothfield, L., A. Taghbalout, and Y. L. Shih.** 2005. Spatial control of bacterial division-site placement. Nat. Rev. Microbiol. **3:**959–968.

59. **Sambrook, J., E. F. Fritsch, and T. Maniatis.** 1989. Molecular cloning: a laboratory manual, 2nd ed. Cold Spring Harbor Laboratory Press, Cold Spring Harbor, NY.

60. **Sandstrom, G., S. Lofgren, and A. Tarnvik.** 1988. A capsule-deficient mutant of *Francisella tularensis* LVS exhibits enhanced sensitivity to killing by serum but diminished sensitivity to killing by polymorphonuclear leukocytes. Infect. Immun. **56:**1194–1202.

61. **Sandstrom, G., A. Sjostedt, T. Johansson, K. Kuoppa, and J. C. Williams.** 1992. Immunogenicity and toxicity of lipopolysaccharide from *Francisella tularensis* LVS. FEMS Microbiol. Immunol. **5:**201–210.

62. **Santic, M., M. Molmeret, K. E. Klose, and Y. Abu Kwaik.** 2006. *Francisella tularensis* travels a novel, twisted road within macrophages. Trends Microbiol. **14:**37–44.

63. **Santic, M., M. Molmeret, K. E. Klose, S. Jones, and Y. A. Kwaik.** 2005. The Francisella tularensis pathogenicity island protein IglC and its regulator MglA are essential for modulating phagosome biogenesis and subsequent bacterial escape into the cytoplasm. Cell. Microbiol. **7:**969–979.

64. **Sjostedt, A.** 2003. Virulence determinants and protective antigens of Francisella tularensis. Curr. Opin. Microbiol. **6:**66–71.

65. **Sjostedt, A., G. Sandstrom, A. Tarnvik, and B. Jaurin.** 1989. Molecular cloning and expression of a T-cell stimulating membrane protein of Francisella tularensis. Microb. Pathog **6:**403–414.

66. **Sjostedt, A., G. Sandstrom, A. Tarnvik, and B. Jaurin.** 1990. Nucleotide sequence and T cell epitopes of a membrane protein of *Francisella tularensis*. J. Immunol. **145:**311–317.

67. **Sorokin, V. M., N. V. Pavlovich, and L. A. Prozorova.** 1996. Francisella tularensis resistance to bactericidal action of normal human serum. FEMS Immunol. Med. Microbiol. **13:**249–252.

68. **Takami, H., Y. Takaki, and I. Uchiyama.** 2002. Genome sequence of Oceanobacillus iheyensis isolated from the Iheya Ridge and its unexpected adaptive capabilities to extreme environments. Nucleic Acids Res. **30:**3927–3935.

69. **Telepnev, M., I. Golovliov, T. Grundstrom, A. Tarnvik, and A. Sjostedt.** 2003. Francisella tularensis inhibits Toll-like receptor-mediated activation of intracellular signalling and secretion of TNF-α and IL-1 from murine macrophages. Cell. Microbiol. **5:**41–51.

70. **Telepnev, M., I. Golovliov, and A. Sjostedt.** 2005. Francisella tularensis LVS initially activates but subsequently down-regulates intracellular signaling and cytokine secretion in mouse monocytic and human peripheral blood mononuclear cells. Microb. Pathog. **38:**239–247.

71. **Tempel, R., X. H. Lai, L. Crosa, B. Kozlowicz, and F. Heffron.** 2006. Attenuated *Francisella novicida* transposon mutants protect mice against wild-type challenge. Infect. Immun. **74:**5095–5105.

72. **Thomas, R. M., R. W. Titball, P. C. Oyston, K. Griffin, E. Waters, P. G. Hitchen, S. L. Michell, I. D. Grice, J. C. Wilson, and J. L. Prior.** 2007. The immunologically distinct O antigens from *Francisella tularensis* subspecies *tularensis* and *Francisella novicida* are both virulence determinants and protective antigens. Infect. Immun. **75:**371–378.

73. **Twine, S., M. Bystrom, W. Chen, M. Forsman, I. Golovliov, A. Johansson, J. Kelly, H. Lindgren, K. Svensson, C. Zingmark, W. Conlan, and A. Sjostedt.** 2005. A mutant of *Francisella tularensis* strain SCHU S4 lacking the ability to express a 58-kilodalton protein is attenuated for virulence and is an effective live vaccine. Infect. Immun. **73:**8345–8352.

74. **Vinogradov, E. V., A. S. Shashkov, Y. A. Knirel, N. K. Kochetkov, N. V. Tochtamysheva, S. F. Averin, O. V. Goncharova, and V. S. Khlebnikov.** 1991. Structure of the O-antigen of Francisella tularensis strain 15. Carbohydr. Res. **214:**289–297.